
This is an electronic reprint of the original article.
This reprint may differ from the original in pagination and typographic detail.

Landman, Rinat; Jämsä-Jounela, Sirkka-Liisa

Hybrid causal analysis combining a nonparametric multiplicative regression causality estimator

Published in:
Control Engineering Practice

DOI:
[10.1016/j.conengprac.2019.104140](https://doi.org/10.1016/j.conengprac.2019.104140)

Published: 01/01/2019

Document Version
Publisher's PDF, also known as Version of record

Published under the following license:
CC BY-NC-ND

Please cite the original version:
Landman, R., & Jämsä-Jounela, S.-L. (2019). Hybrid causal analysis combining a nonparametric multiplicative regression causality estimator. *Control Engineering Practice*, 93, Article 104140.
<https://doi.org/10.1016/j.conengprac.2019.104140>

This material is protected by copyright and other intellectual property rights, and duplication or sale of all or part of any of the repository collections is not permitted, except that material may be duplicated by you for your research use or educational purposes in electronic or print form. You must obtain permission for any other use. Electronic or print copies may not be offered, whether for sale or otherwise to anyone who is not an authorised user.



Hybrid causal analysis combining a nonparametric multiplicative regression causality estimator with process connectivity information



R. Landman*, S.-L. Jämsä-Jounela

Aalto University, School of Chemical Technology, Process Control and Automation Research Group, P.O. Box 16100, FI-00076 Espoo, Finland

ARTICLE INFO

Keywords:

Nonparametric multiplicative regression
Causality analysis
Process connectivity
Fault propagation
Board machine

ABSTRACT

Industrial processes are often subjected to abnormal events such as faults or external disturbances which can easily propagate via the process units. Establishing causal dependencies among process measurements has a key role in fault diagnosis due to its ability to identify the root cause of a fault and its propagation path. This paper proposes a hybrid nonlinear causal analysis based on nonparametric multiplicative regression (NPMR) for identifying the propagation of an oscillatory disturbance via control loops. The NPMR causality estimator addresses most of the limitations of the linear model-based methods and it can be applied to both bivariate and multivariate estimations without any modifications to the method parameters. Moreover, the NPMR-based estimations can be used to pinpoint the root cause of a fault. The process connectivity information is automatically integrated into the causal analysis using a specialized search algorithm. Thereby, it enables to efficiently tackle industrial systems with a high level of connectivity and enhance the quality of the results. The proposed approach is successfully demonstrated on an industrial board machine exhibiting oscillations in its drying section due to valve stiction and. The NPMR-based estimator produced highly accurate results with relatively low computational effort compared with the linear Granger causality and other nonlinear causality estimators.

1. Introduction

Owing to the increasing demand for a higher product capacity and quality, energy efficient and safe operations, the spreading of faults and disturbances in large-scale systems is a major concern. Different faults such as undesired parameter changes, sensor and actuator problems can easily propagate through the process components by material or information flows and degrade the process performance (Yang & Xiao, 2012). Therefore, there is a constant need in developing fault detection and diagnosis methods to efficiently handle abnormal events (Venkatasubramanian, Rengaswamy, Yin, & Kavuri, 2003). In particular, multivariate statistical process monitoring methods have become increasingly popular in the field of process monitoring due to their simplicity and the emergence of Industry 4.0 (Zhao & Sun, 2019).

For closed-loop processes, disturbances caused by normal operating condition changes can be compensated and the manipulated variables may be eventually controlled around their new set-points. However, in case of real process faults, dynamic variations may be observed since the disturbance cannot be compensated (Li, Zhao, & Huang, 2018). This is the case when friction in a valve causes a limit-cycle oscillation in control loops (Thornhill, Cox, & Paulonis, 2003). As the control loops in an industrial plant are interconnected to each other; oscillations can easily propagate through the control-loops of a process ultimately

leading to poor control performance and excessive energy consumption (Duan, Chen, Shah, & Yang, 2014; Yuan & Qin, 2013). Therefore, it is eminently important to distinguish the root cause from the consequent oscillations to allow optimal operating conditions (Choudhury et al., 2007; Duan et al., 2014).

Causality analysis offers a practical tool to retrace a fault propagation path and its root cause by capturing the cause and effect relationships between process variables. Causality can be captured from process knowledge and/or data (Duan et al., 2014; Yang, Duan, Shah, & Chen, 2014). A qualitative model of a system can be obtained by utilizing expert knowledge, e.g., in the form of first principle mathematical models or alternatively it can be extracted from a graphical representation of a process such as piping and instrumentation diagram (P&ID) or process flow diagram (PFD) (Yang et al., 2014). P&IDs are available in a standardized electronic form (XML) via several commercial CAD tools. The connectivity information can be captured from those tools as open XML text which describes the process schematic that complies with Computer Aided Engineering Exchange (CAEX) schema (Thambirajah, Benabbas, Bauer, & Thornhill, 2009).

However, models based on process knowledge have their inherent limitation of being qualitative and relying on prior process knowledge which is not always available (Duan et al., 2014; Duan, Yang,

* Corresponding author.

E-mail address: rinat.landman@aalto.fi (R. Landman).

Chen, & Shah, 2013). On the other hand, data-driven analysis offers a practical approach to obtain a quantitative measure of causality by utilizing historical process data in the form of time series that is often readily available in industrial systems. Popular data-based methods are cross-correlation analysis (Bauer & Thornhill, 2008), frequency domain methods such as direct transfer function (DTF) (Kaminski & Blinowska, 1991) and partial directed coherence (PDC) (Baccala & Sameshima, 2001), Granger causality (GC) (Granger, 1969), transfer entropy (TE) (Schreiber, 2000) and nearest neighbors (Bauer, Cox, Caviness, Downs, & Thornhill, 2007).

Each of the data-based methods has its own limitations and advantages (Duan et al., 2014; Yang & Xiao, 2012). GC and the frequency domain methods are based on auto-regressive (AR) modeling, therefore they rely on the model accuracy and are restricted to linear causality. Several extensions to GC based on non-linear model identification have been proposed in order to detect causality (Chen, Rangarajan, Feng, & Ding, 2004; Faes, Nollo, & Chon, 2008), however, those extensions remain parametric and rely on AR model fitting (Nicolaou & Constandinou, 2016). Other non-linear approaches to GC suggest replacing the traditional AR modeling with a Gaussian model such as radial basis Function (RBF) (Ancona, Marinazzo, & Stramaglia, 2004; Chen, Zhao, Yan, & Yao, 2017), however, those models remain parametric and their application to multivariate estimations is not addressed.

TE is a nonlinear method, however, it is more computationally heavy compared with the linear methods since it requires estimation of multidimensional probability density function (PDF). In addition, it requires estimation of several parameters such as embedding dimension and time delay whose selection is a tradeoff between the accuracy of the results and the computational burden (Duan et al., 2014; Landman & Jämsä-Jounela, 2016). Although several multivariate extensions have been proposed to GC and TE (Chen et al., 2004; Duan et al., 2013; Guo, Seth, Kendrick, Zhou, & Feng, 2008; Vakorin, Krakovska, & McIntosh, 2009), methods such as nearest neighbors and cross-correlation are restricted to bivariate analysis.

Recently, a new causality estimator based on nonparametric multiplicative regression (NPMR) was proposed by Nicolaou and Constandinou (2016). The concept of NPMR originates from the area of ecology and was first introduced in the context of habitat modeling (McCune, 2006, 2011).

NPMR-based estimator offers several advantages over the traditional causality methodologies: it is nonparametric, i.e., it does not rely on estimation of any type of parametric model. It can be applied to both linear and non-linear systems and there is no restriction on the order of nonlinearity that can be estimated. Furthermore, the estimator can be used for both pairwise and multivariate estimations without any modifications (Nicolaou & Constandinou, 2016). The inherent features of NPMR eliminate any overfitting issues, a problem which often leads to detection of spurious causalities when using other nonlinear methods (Palus & Vejmelka, 2007). All these features of the estimator combined with the following procedures make it explicitly appealing for industrial applications: (1) statistical significance can be tested using surrogate data; (2) the sensitivity measure Q can be used to evaluate the contribution of particular parameters within the model (Nicolaou & Constandinou, 2016).

In this paper we propose to combine a causality estimator based on NPMR with the information on process connectivity in order to provide a powerful diagnostic tool which can efficiently tackle complex industrial processes. Recent studies (Bauer, Thornhill, & Meaburn, 2005; Duan et al., 2014; Thambirajah, Benabbas, Bauer, & Thornhill, 2007; Yang, Shah, & Xiao, 2012) highlight the need to utilize process insights derived from process schematic or site expertise in order to validate the results of the data-based methods. In particular, this approach is beneficial when investigating a complex system with multiple bidirectional and/or recycle streams. Consequently, several attempts have been made to develop an automated tool for diagnosis of plant-wide disturbances by combining data-based methods with process

connectivity information. Moreover, the possibility for an automatic extraction of the process connectivity information and integrating it with data-based analysis generates an effective and powerful diagnostic tool (Duan et al., 2014; Thornhill & Horsch, 2007). (Yim et al., 2006) developed a software named plant-wide disturbance analysis (PDA) which given an electronic P&ID and results from a data-based analysis, allows the user to perform queries about the plant and detect the root cause of disturbances. Furthermore, Thambirajah et al. (2009) introduced a cause-and-effect analyzer which combines a data-based analysis with the process connectivity information derived from an XML description of a process schematic. The cause-and-effect analyzer searches through the connectivity matrix representing a schematic of a chemical process to find paths by which disturbances can propagate through the process. However, these studies focus on searching for feasible propagation paths between process elements for validating the results of a data-based analysis or identifying a root cause of a fault. In complex systems with numerous bidirectional and recycle streams, finding feasible propagation paths between process components might not be sufficient to obtain an accurate causal model. This study proposes a hybrid causal analysis which aims to reduce the number of spurious results obtained from the data-based analysis while simultaneously minimizing the computational burden throughout the analysis. This is achieved by estimating the causality between each of the measurement points based on the physical connectivity among them: bivariate estimation for direct connectivity and multivariate estimation for indirect connectivity.

The cornerstone of the causal analysis is a specialized search algorithm based on a depth-first search (Thambirajah et al., 2009). The search algorithm has two functionalities: finding feasible propagation paths between control elements and determine whether each path is direct or indirect based on the process topology. The ability of the search algorithm to determine whether a physical path between two controllers is direct or indirect facilitates the analysis and reduces the results of the data-based causal analysis which do not represent direct causality. Moreover, this study proposes a measure for identifying the root cause of a fault using the NPMR-based causality estimations.

The analysis is executed according to the following procedure. Initially, the process connectivity information is extracted in the form of an adjacency matrix (Jiang, Patwardhan, & Shah, 2008) which is captured from an XML scheme using AutoCAD P&ID (Landman, Kortela, Sun, & Jämsä-Jounela, 2014; Thambirajah et al., 2009). Then, the bivariate NPMR-based causality is estimated for all paths which are considered as direct based on the process topology while the conditional (multivariate) NPMR-based causality is calculated for each indirect path and the maximum value is considered as a causality measure. This methodology is exemplified in this paper using a case study of an industrial board machine with multiple oscillating control loops due to valve stiction. This highly inter-connected system serves to illustrate the effectiveness and the advantages of the proposed hybrid analysis. The results are discussed and the NPMR-based estimator is evaluated against other causality estimators. Furthermore, since the causal model points on two possible root causes for the fault, a straightforward method is proposed for locating the root cause by utilizing the causality matrix.

This paper is structured as follows. In Section 2 the proposed NPMR-based causality framework is explained in detail including all the methods which are part of the analysis. A description of an industrial case study is given in Section 3. Next, the data preparation and the procedure for setting the parameters are described in detail. Finally, the results are presented and evaluated and the NPMR-based estimator is compared to other causality estimators. The paper ends with summary and conclusions in Section 4.

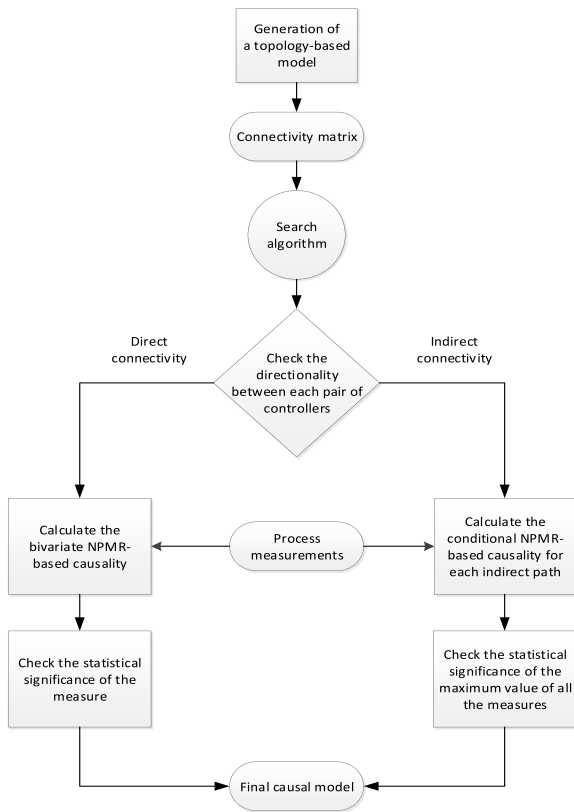


Fig. 1. The analysis framework based on the NPMR-based causality estimator.

2. The NPMR-based causality analysis framework

The study aims to identify the propagation path of oscillation through control loops. The analysis consists of the following steps: first, the connectivity information is extracted from the P&ID of the process. Next, the NPMR-based causality is estimated between each pair of controllers based on their directionality. Namely, the search algorithm searches for feasible propagation paths between each pair of control loops. Then, if such paths exist, the search algorithm checks whether the controllers are connected directly or indirectly. According to Jiang et al. (2008), a direct path from controller i to controller j exists if the output of controller i has a direct effect on the output of controller j without any intermediate effect on any other controller. Respectively, the search algorithm identifies a physical pathway between controllers i and j as direct if it does not traverse any control element which does not belong to either i or j controllers.

If two controllers are directly connected, the bivariate NPMR-based causality is estimated while if the controllers are connected indirectly, the conditional (multivariate) NPMR-based causality is calculated for all the indirect paths and the maximum value is taken as a directionality measure. Finally, all the estimations undergo a statistical evaluation using surrogate data. The overall framework for the causal analysis is illustrated in Fig. 1 while the explicit logic for calculating the NPMR-based causality measure with the search algorithm is presented in Fig. 2.

In the following subsections, the procedure for capturing the connectivity information, the logic of the search algorithm and the NPMR-based causality estimator are described in detail.

2.1. Extracting the connectivity information

Connectivity information describes the physical linkage between process components. It can be extracted from P&IDs or PFDs and

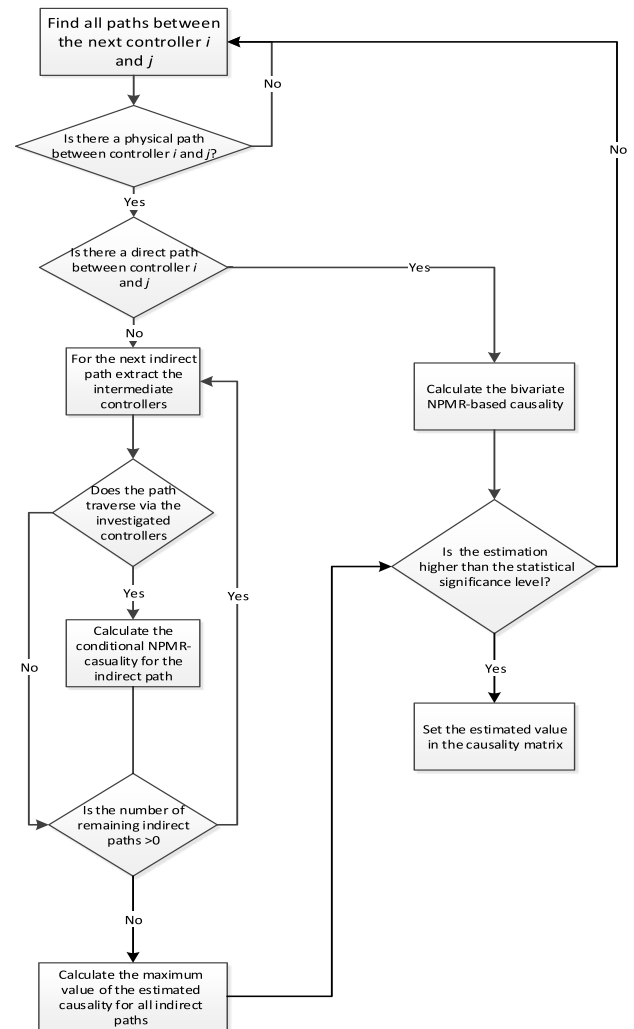


Fig. 2. The logic of calculating the NPMR-based causality throughout the analysis.

then converted into a causal digraph or a connectivity (adjacency) matrix. Yang et al. (2014) The digraph and the connectivity matrix are a graphical and numerical representation of the process topology, respectively (Sun, 2013).

The process schematic can be converted into eXtensible Markup Language (XML). XML is a scripting language that describes the equipment, their properties and the connections among them while ensuring that it can be interpreted by both humans and computers (Thambirajah et al., 2009; Yim et al., 2006). In this work, the connectivity information was extracted from an electronic P&ID drawn by a specialized Autodesk AutoCAD drafting application and the topology data was exported in the format of ISO-15926-compliant XML scheme XMpLant (Landman et al., 2014; Noumenon, 2008). The connectivity information, i.e., the properties of the process components and the connections among them were extracted via the database object of the drawing. This information was further processed using object oriented programming (OOP) tool of MATLAB in order to obtain a connectivity matrix, whose elements are set to '1' in case of a direct connectivity and otherwise '0' (Landman et al., 2014).

2.2. Finding physical pathways using a search algorithm

The search algorithm was developed to have the following three functionalities: (1) detect whether there is a physical pathway between two controllers corresponding to each 'cause' and 'effect' controllers.

(2) Determine whether the path is direct or indirect. (3) In case a path is indirect, the algorithm returns the intermediate controllers between the ‘cause’ and ‘effect’ controllers. The first two functionalities determine the type of causality to be estimated according to the logic presented in Fig. 2.

First, the algorithm searches for all possible propagation paths starting at the ‘cause’ variable leading to the ‘effect’ variable. In this case, the variables correspond to the measurement elements (i.e., indicators) of each control loop. The search is based on a graph traversal algorithm which searches through series of nodes (corresponding to the control elements) while ensuring that each node is traversed only once (Thambirajah et al., 2009). In this case, the algorithm ‘searches’ through the connectivity matrix to find elements which are physically connected via pipe-lines or signal lines. The underlying idea of the search algorithm is to move from the element connected to the ‘cause’ variable and search for columns with ‘1’s which indicate that the row element is directly connected to the column element. This procedure continues repetitively until the same element is visited twice or the row element disconnected from any elements. Then, the algorithm backtracks to ensure all possible pathways are found (Thambirajah et al., 2009).

Once all possible propagation paths between each pair of elements are found, the algorithm checks whether each path is direct or indirect. If a path from controller i to controller j traverses only equipment elements or control elements which belong to either i or j control loops it is considered as direct. Otherwise, if a path traverses control elements which belong to neither i or j controllers, the path is considered as indirect (Landman et al., 2014).

2.3. NPMR-based causality estimator

Nicolaou and Constandinou (2016) extended the basic NPMR (McCune, 2006) to handle applications outside of habitat modeling, in particular, causality estimation. The basic idea of NPMR is as follows. Consider a response variable Y with N samples: $Y = [y_1, y_2, \dots, y_N]$ and consider a matrix X with m predictors:

$$X = \begin{pmatrix} x_{1,1} & x_{1,2} & \dots & x_{1,m} \\ x_{2,1} & x_{2,2} & \dots & x_{2,m} \\ \vdots & \vdots & \ddots & \vdots \\ x_{N,1} & x_{N,2} & \dots & x_{N,m} \end{pmatrix} \quad (1)$$

Next, a response surface of y is built from its m predictors using a multiplicative kernel smoother (McCune, 2006). This is achieved by estimating each value y_n , ($n = 1, \dots, N$) from its local neighborhood corresponding to the predictor space $X_n = [x_{n,1}, x_{n,2}, \dots, x_{n,m}]$. The influence of each predictor X_j , ($j = 1, \dots, m$) on the estimation is defined by its corresponding tolerance of the kernel smoother, σ_j , which is a unique feature for NPMR (McCune, 2006; Nicolaou & Constandinou, 2016). In this study, the local neighborhood is defined as the weighted mean and the weights are estimated using a Gaussian weighting function (Eq. (2)). The weights are the distances of each of the m predictors from a target point X_n scaled by the standard deviation (tolerance) of each predictor.

$$w_{i,j} = e^{-\frac{1}{2}[(x_{i,j} - x_{n,j})/\sigma_j]^2} \quad (2)$$

The Gaussian kernel is a simple and intuitive way to express the distance of a point from its target point. The Gaussian kernel tolerance defines how broadly the information from the local neighborhood in the predictor space is taken in order to estimate the value at the target point (McCune, 2006). The Gaussian kernel allows the weights to smoothly decrease as the distance of the samples from the target point increases and the rate at which the weights are decreased can be adjusted by modifying the tolerance (McCune, 2006; Nicolaou & Constandinou, 2016). Thereupon, the estimation of target point n of y can be obtained as follows:

$$\hat{y}_n = \frac{\sum_{i=1, i \neq n}^N y_i (\prod_{j=1}^m w_{i,j})}{\sum_{i=1, i \neq n}^N (\prod_{j=1}^m w_{i,j})} \quad (3)$$

The estimate is the mean value of the observations where each observation is weighted according to its distance from the target point in the predictor space with the weights being the product of the individual weights. By omitting the target point n from the estimation, overfitting is avoided and error estimates are more realistic (McCune, 2006). A detailed example of NPMR for a small dataset is provided by McCune (2011).

The basic idea of NPMR was formulated in the context of causality estimation by extending the predictor space to include past information as additional predictors (Nicolaou & Constandinou, 2016). This is achieved by using time delayed embedded vectors of the predictor variables. For time instance n , the embedded vector \tilde{x}_n is defined as $\tilde{x}_n = [x_n, x_{n-\tau}, \dots, x_{n-(d-1)\tau}]$ where d is the embedded dimension and τ is the embedding time delay. By using embedded vectors as predictors, past information is included in the prediction of y . The variance of the modeling error indicates how accurate the estimation is. The bivariate NPMR-based causality estimator is defined as follows:

$$C_{NPMR}(X_j \rightarrow Y) = \log \left(\frac{\sigma_{(Y,\tilde{Y})}^2}{\sigma_{(Y,(\tilde{Y},\tilde{X}_j))}^2} \right) \quad (4)$$

where \tilde{X}_j is the time-delayed matrix of the j th predictor, \tilde{Y} is the time-delayed matrix of the response variable Y . $\sigma_{(Y,\tilde{Y})}^2$ and $\sigma_{(Y,(\tilde{Y},\tilde{X}_j))}^2$ are the error variances when past values of Y are used as predictors and when both past values of Y and X_j are used as predictors, respectively. Eq. (4) is analogous to the definition of the traditional GC where the numerator corresponds to the residuals of the restricted model while the denominator corresponds to the residuals of the unrestricted model (Bressler & Seth, 2011). Likewise, the conditional C_{NPMR} follows the definition of the conditional GC (Guo et al., 2008):

$$C_{NPMR}(X_j \rightarrow Y/Z) = \log \left(\frac{\sigma_{(Y,\tilde{Y},Z)}^2}{\sigma_{(Y,(\tilde{Y},\tilde{X}_j,Z))}^2} \right) \quad (5)$$

where Z corresponds to the intermediate variables, excluding X_j . Negative values of C_{NPMR} imply that including the past information on the predictors results in a worse model fit, i.e., there is no causal dependency among the time series.

The relative contribution of each predictor can be estimated with sensitivity analysis. Sensitivity analysis involves adding and subtracting a small proportion from each predictor j and evaluating the resulting change in the estimated prediction. The sensitivity, Q , is measured as follows (Nicolaou & Constandinou, 2016):

$$Q(Y/X_j) = \frac{\sum_{i=1}^N |\hat{y}_i^+ - \hat{y}_i| + |\hat{y}_i^- - \hat{y}_i|}{2N|y_{max} - y_{min}|\Delta} \quad (6)$$

where y_{max} and y_{min} are the maximum and minimum values of Y , respectively, \hat{y}_i is the estimated value of y_i without cross validation. \hat{y}_i^+ and \hat{y}_i^- are the estimated response when increasing and decreasing X_j by an arbitrary small proportion, respectively (estimated without cross-validation). Δ is a small proportion by which each predictor is nudged. Large values of Q indicate on high sensitivity to the response to the particular predictor.

In addition, the overall model fit can be evaluated via ‘‘cross R^2 ’’ (McCune, 2011):

$$\chi R^2 = 1 - \frac{RSS}{TSS} = 1 - \frac{\sum_{i=1}^N (y_i - \hat{y}_i)^2}{\sum_{i=1}^N (y_i - \bar{y}_i)^2} \quad (7)$$

where y_i is the predicted variable, \hat{y}_i is the estimated variable calculated according to Eq. (3) and \bar{y}_i is the mean of the predicted variable. The model fit is evaluated based on the relationship between the residual sum of squares (RSS) and the total sum of squares (TSS). A value of χR^2 which is close to 1 indicates on a good model fit.

2.3.1. Statistical significance

The statistical significance of each $C_{NPMR}(x \rightarrow y)$ can be estimated with surrogate data. If a $C_{NPMR}(x \rightarrow y)$ is higher than its threshold significance level, causality from x to y can be deduced. Surrogate time series have the same power-spectrum, auto-correlation function and probability density function as the original series, with the exception of the phases and frequencies being randomized (Bauer et al., 2007). There are several methods to generate surrogate data and in this study the amplitude adjusted Fourier transform (AAFT) method was used (Theiler, Eubank, Longtin, Galdrikian, & Farmer, 1992). The key steps of the AAFT algorithm are as follows: (1) The original data is rescaled to a normal distribution by generating time series with Gaussian white noise and sorting them according to the ranking of the original series. (2) The rescaled data is Fourier transformed and the phase component is randomized. (3) The surrogates are scaled to the distribution of the original data using the inverse Fourier transform (Bauer et al., 2007; Dolan & Spano, 2001).

The number of surrogates for a particular statistical level can be estimated via $N_{surr} = \frac{1}{\alpha} - 1$ where α is the desired statistical significance (Nicolaou & Constandinou, 2016). Bauer et al. (2007) suggest that 20 surrogates should provide statistically relevant results while maintaining a reasonable computational effort. Consequently, in this study 20 surrogates were generated for each causality estimation, i.e., $\alpha \approx 0.05$ in order to obtain a 95% significance level.

For each pair of surrogates, the NPMR-based causality estimator is applied and the significance level is set to be the maximum value of C_{NPMR} of all estimations.

2.3.2. Parameters settings

An appropriate selection of time delay allows longer dynamics to be taken into account in the estimation (Nicolaou & Constandinou, 2016). The minimum embedding dimension is dependent on the time delay τ , hence the delay should be selected before the embedding dimension is determined (Cao, 1997). Various methods have been proposed to for estimating the time delay. For instance, the criteria can be based on the minimum of mutual information (Fraser & Swinney, 1986) or when the auto-correlation function approaches zero (Nicolaou & Constandinou, 2016).

Nicolaou and Constandinou (2016) suggest that the embedding dimension does not affect the pattern of the causality but rather its amplitude, yet, it is recommended to select the appropriate embedding dimension using any method provided in literature. A practical approach for estimating the minimum embedding dimension was proposed by Cao (1997). Alternatively, the model fit (Eq. (7)) can be used to determine the minimum embedding dimension by selecting a threshold for model fit improvement when increasing the embedding dimension (McCune, 2011; Nicolaou & Constandinou, 2016).

Lastly, the tolerance factor can be optimized via an iterative procedure or it can be estimated from the data itself (McCune, 2011; Nicolaou & Constandinou, 2016). One of the advantages of NPMR is that it allows for each predictor to have a different tolerance, i.e., the influence of each predictor in the estimation can be adjusted (Nicolaou & Constandinou, 2016).

3. Industrial case study: valve stiction in a board machine

The process case study involves an industrial board machine producing various liquid packaging. The aim of this investigation is to identify the propagation path of oscillation which originates in the drying section of the machine due to valve stiction. Valve stiction is one of the main causes for valve malfunctions in the board machine, in particular, the drying section where it affects the control loops (Jämsä-Jounela et al., 2012; Pozo Garcia, Tikka, Zakharov, & Jämsä-Jounela, 2013). Oscillations generated by valve stiction can propagate to different parts of the machine due to the high connectivity between the controllers in drying section and ultimately affect the board quality

and undermine the process performance (Pozo Garcia et al., 2013). The analysis consists of the following steps: first, the data is pre-processed and the subset of variables for the analysis is selected. Next, the parameters of the NPMR-based estimator are selected. Finally, the causal analysis is carried out based on the selected parameters according to the steps presented in Fig. 2. In the following subsections the process case study is described, the procedure for preparing the data and setting the parameters is explained and the results are discussed and evaluated. Furthermore, a procedure for identifying the root cause of the fault is proposed and the performance of the NPMR-based estimator is compared to other causality estimators based on several criteria.

3.1. The drying section

The main purpose of the drying section is to evaporate the water that remains in the paper web in order to obtain the desired moisture content in the board. This is achieved by heating the paper web with steam-filled cylinders. The condensation of the steam releases latent heat which evaporates the water in the paper. The scheme of the process is shown in Fig. 3. The drying section contains six consecutive drying groups containing in total 74 cylinders. Each drying group consists of a steam group of drying cylinders and a condensate tank where the condensate is collected. Each drying group has its own controllers to control the steam pressure, the pressure difference between the steam and condensate headers and the level of the condensate tanks. The steam to the cylinders is supplied by 5 and/or 10 bar steam headers (denoted as red pipes at the top of Fig. 3). The pressure difference is controlled by regulating the steam outlet of the condensate tanks and the level at the condensate tanks is controlled by manipulating the flow outlet valve. The investigated case study involves valve stiction which originates in PC1652, the pressure controller of steam group 3.

The stiction was detected using the valve stiction detection system proposed by Zakharov, Zattoni, Xie, Pozo Garcia, and Jämsä-Jounela (2013) and was subsequently confirmed by the long-term maintenance log books of the plant.

3.2. Dataset preparation

The measured process variables (PVs) corresponding to each controller are presented in Fig. 4. In total, there are 22 process measurements in the drying section measured with a sampling interval of 10 s ($F_s = 0.1$ Hz). Initially, the series were normalized to zero mean and scaled to a unit standard deviation. Next, in order to reduce the dimensionality of the analysis it was essential to select the variables which are most pertinent to the fault. This step does not only reduce the complexity of the analysis, but it also enhances the results and facilitates their interpretation (Yuan & Qin, 2013). Several clustering methods are reported in literature for isolating faulty variables for diagnostic purposes, e.g., principal component analysis (Yuan & Qin, 2013; Zhao & Wang, 2016), spectral and oscillation analysis (Bauer et al., 2005), spectral envelope method (Duan et al., 2014), variable selection method using least absolute shrinkage and selection operator (Yan & Yao, 2015), reconstruction-based contribution method (Alcala & Qin, 2009; Li, Qin, & Yuan, 2016), sparse exponential discriminant analysis (Yu & Zhao, 2018) and more.

Due to the oscillatory behavior of the control loops, spectral analysis was chosen to identify series with similar features. Power spectra are invariant to phase of a signal, meaning they are insensitive to the time delays between one series and another (Bauer et al., 2005).

The spectra (Fig. 5) reveals that the series that share the same oscillation frequency (0.007 Hz) are PC668, PC1653, PC651, PC652, PC653, PC670, LC652, PC1652, PC671, LC653, PC672 and PC673. The NPMR-based estimator does not require the data to be stationary, therefore, longer segments of data can be analyzed to obtain a robust model and capture longer dynamics (Nicolaou & Constandinou, 2016). However, the amount of data also affects the computational load. Consequently, 1000 samples (from 1000 to 2000) were taken for the analysis.

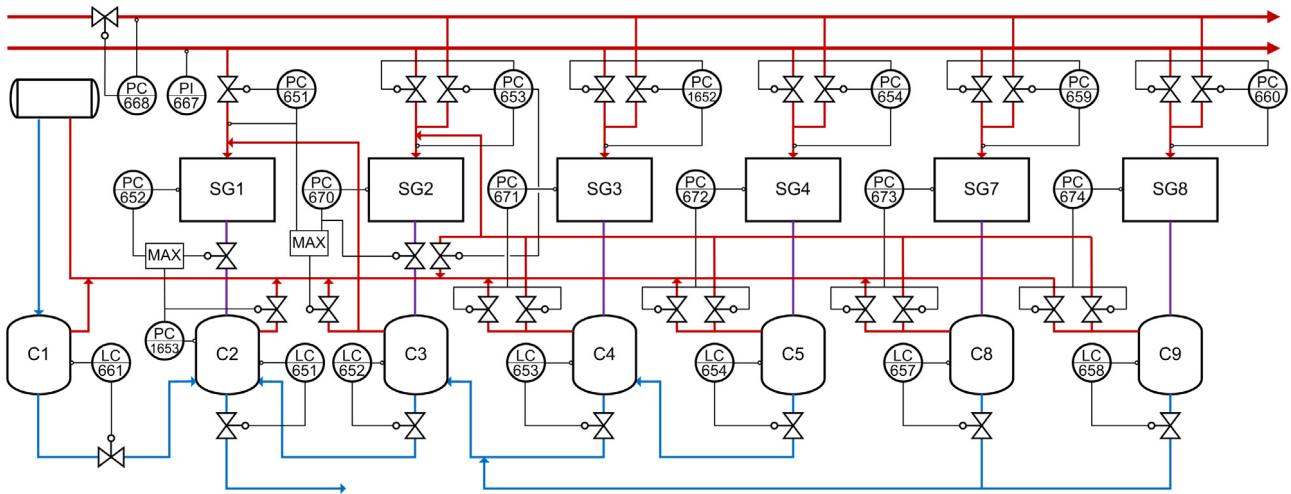


Fig. 3. Flow sheet of the drying section. Red lines indicate steam pipes, blue lines indicate condensate pipes and purple lines indicate mixed flow of steam and condensate (PI = pressure indicator, PC = pressure controller, LC = level controller, SG = steam group, C = condensate tank). (For interpretation of the references to color in this figure legend, the reader is referred to the web version of this article.)

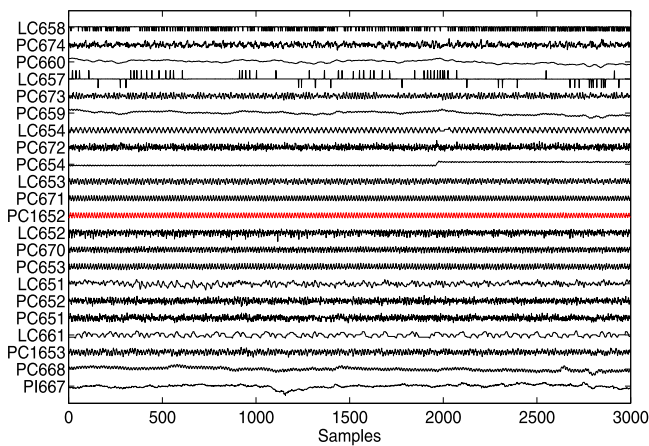


Fig. 4. The measured process variables (PVs). The oscillation originates in PC1652 (in red). (For interpretation of the references to color in this figure legend, the reader is referred to the web version of this article.)

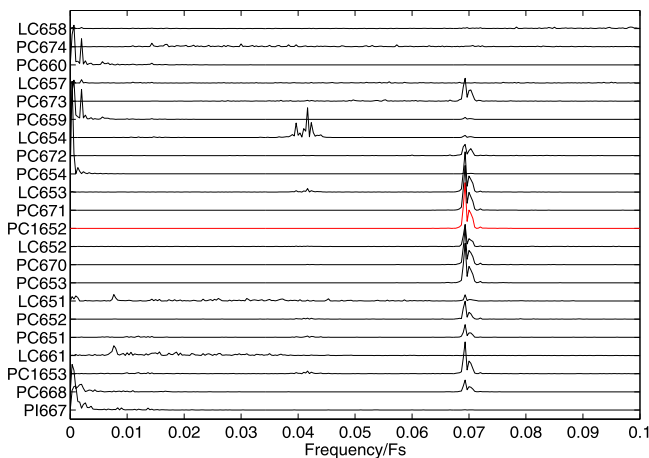


Fig. 5. The spectra of the process variables (Fs = 0.1 Hz). The oscillation originates in PC1652 (in red). (For interpretation of the references to color in this figure legend, the reader is referred to the web version of this article.)

3.3. The procedure for parameters settings

First, the time delay, τ , was estimated as the time when the auto-correlation function reaches $1/e$ (Nicolau & Constantinou, 2016). The estimated time delay for the majority of the series was 3 and for the remaining ones it was 2, therefore, τ was set to 3 for all the series. Next, the embedding dimension was evaluated according to the method presented by Cao (1997). For each $d = 1, 2, \dots, 10$ and $\tau = 3$ the values of $E1$ and $E2$ were calculated. The results revealed that the minimum embedding dimension (i.e., the minimum d for which $E1$ and $E2$ stop changing) varied between 2–4 and therefore it was decided to set $d = 4$ throughout the whole analysis. Sensitivity analysis can also be used in order to tune some of the parameters or as an additional measure for supporting the selection of a certain parameter. For instance, by checking the sensitivity of a predicted value to different lagged samples of a certain predictor one can examine the influence of d and τ on the estimated value.

Finally, the kernel tolerance (σ) was tuned for each pair of series by calculating the model fit for $\sigma = 0.2, 0.4, 0.6, \dots, 2$ and $\tau = 3, d = 4$. The tolerance which produced the best model fit for each pair was selected. The estimation of \hat{y}_i in Eq. (7) was calculated by considering every X_j as a predictor. The results showed a slight variation in the optimum value of σ for each pair of series ($0.2 < \sigma < 0.8$), hence, an optimum value was set individually for each pair. As an example, Fig. 6 presents the model fit as a function of σ from PC1652 to all other controllers. The best model fit for the majority of the pairs is achieved at low sigma values (0.2–0.8). One interesting finding is that the best model fit (> 0.8) is obtained when predicting the neighboring controllers of PC1652.

3.4. Results

The causality matrix with the calculated $C_{NPMR}(X_i \rightarrow X_j)$ values for each (i, j) th pair of controllers is shown in Table 1. The values were calculated according to the scheme in Fig. 2. Zeros indicate either on lack of physical connectivity or C_{NPMR} values that are lower than their significance level. In addition, negative values of C_{NPMR} were excluded. Table 2 presents the connectivity information according to the search algorithm : empty cells indicate on lack of physical connectivity, squares denote indirect paths and bullets denote direct paths between the row and column controllers.

Overall, the results indicate that all the paths which were identified as indirect by the search algorithm were confirmed as indirect as well

Table 1
The NPMR-based causality matrix with adjusted parameters.

C_{NPMR} _{row-column}	PC1653	PC651	PC652	PC653	PC670	LC652	PC1652	PC671	LC653	PC673
PC1653										
PC651			0.053							
PC652	0.065	0.172								
PC653					0.303					
PC670		0.036	0.078	0.156		0.100				
LC652		0.102	0.058							
PC1652								0.190	0.498	
PC671				0.094	0.134		0.090		0.234	
LC653		0.108	0.249			0.135				
PC673										

Table 2
The connectivity information: indication of direct/indirect paths according to the search algorithm.

	PC1653	PC651	PC652	PC653	PC670	LC652	PC1652	PC671	LC653	PC673
PC1653										
PC651	□		•							
PC652	•									
PC653	□	□	□		•	□				
PC670	◦	•	•	•		•				
LC652	•	•	•							
PC1652	□	□	□	□	□	□		•	•	
PC671	□	□	□	•	•	□	•		•	
LC653	□	•	•	□	□	•				
PC673	□	□	□	•	•	□				

Empty cells denote lack of physical connectivity, squares denote indirect paths and bullets denote direct paths between the row and column elements.

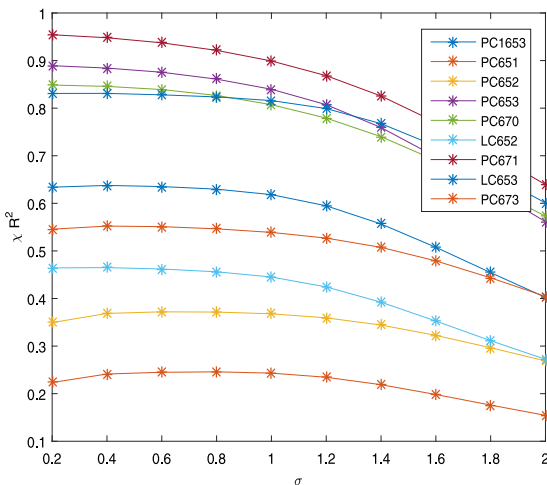


Fig. 6. The model fit from PC1652 to all other controllers for different values of σ with $\tau = 3, d = 4$.

according to the NPMR-based estimator since their corresponding estimations were found to be statistically insignificant; Whilst the majority of the paths which were identified as direct by the search algorithm were confirmed as direct based on their C_{NPMR} values.

In this case, a discrepancy between the physical connectivity and the causality estimation can occur due to one of the following reasons: causality might exist but on a very low level (e.g., LC652 → PC1653) or there is a direct physical path but there is no information transfer due to a closed valve. The latter scenario might be the case for PC673 → PC653 and PC673 → PC670. PC673 manipulates two valves, whereas only one of the valves has direct interaction with PC653 and PC670 via the outlet steam line of C8. Typically, only one valve is constantly open while the second valve is opened only when the controller output exceeds a certain threshold (the pressure controllers are adjusting the steam flow to the cylinders in the same manner). Therefore, if only one valve is open, there is no flow through the other valve which eliminates

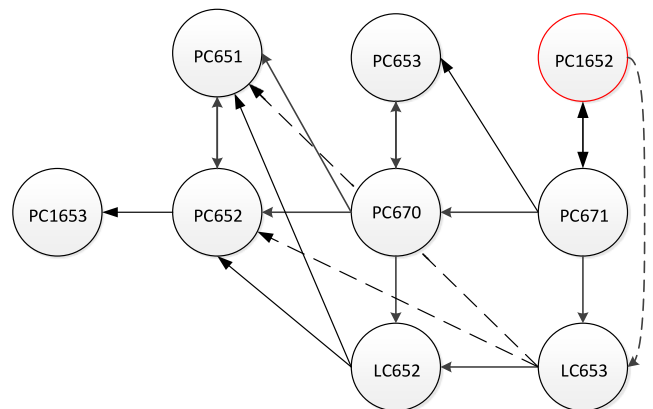


Fig. 7. The causal model according to Table 1 (dashed arcs correspond to causality which is suspected as indirect).

any information transfer to SG2. This scenario exemplifies that physical connectivity does not necessarily imply on causality.

The causal model based on Table 1 is shown in Fig. 7. The paths which are suspected as indirect are denoted as dashed arcs. Initially, the path PC1652 → LC653 is suspected as indirect according to the captured topology (Fig. 7), however, according to the search algorithm the path is direct since the steam condensate from SG3 is transferred directly to C4 (unlike SG2 and SG1 where the pressure difference controllers adjust the steam condensate flow, respectively). Moreover, the high C_{NPMR} value (≈ 0.5) implies on a high level of interaction between PC1652 and LC653. The path from LC653 to controllers PC651 and PC652 is recognized as direct, however, in this case as well, the paths are further investigated to ensure direct causality. The search algorithm reveals that the direct path from LC653 to PC651 and PC652 is via the steam outlet of C3 which flows directly into SG1 (see the output of the search algorithm in Fig. 8), thereby affecting both PC651 and PC652. However, since the bottom flow outlet of C4 initially alters the level in C3, it is reasonable to assume that LC652 is primarily affected by LC653. Consequently, the C_{NPMR} values of LC653 → PC652

Table 3
The indirect paths from LC653 to PC651 and LC652 and their NPMR-based causality estimation.

Indirect Path	C_{NPMR}	Significance level
LC653 → LC652 → PC651	0.051	0.093
LC653 → LC652 → PC652	0.138	0.011

```

*****
Checking cause and effect relationship between LI-653 and PI-651...
LI-653 is connected to
C-4
There is a direct link between C-4 and PI-651...
The direct path is :
    
```

```

Path 1 is
C-4
LI-653
LC-653
LV-653
C-3
SG1_steam_Line
PI-651

Path 2 is
C-4
LV-653
C-3
SG1_steam_Line
PI-651
    
```

Fig. 8. The output of the search algorithm for direct paths from LC653 to PC651. LI = Level Indicator, LC = level Controller, LV = Level Transmitter, PI = Pressure Indicator.

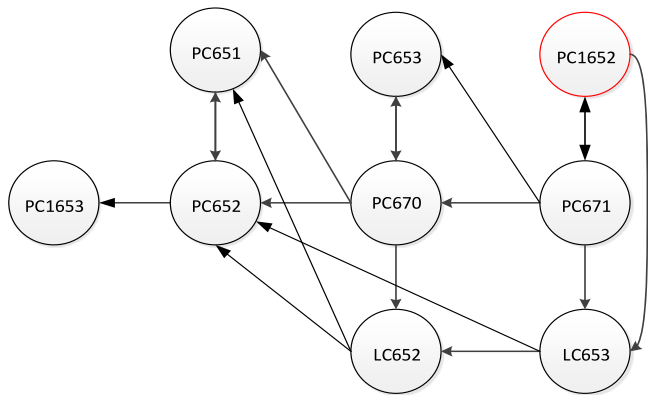


Fig. 9. The final causal model.

and LC653 → PC651 via intermediate controller LC652 are calculated. The results (Table 3) suggest that the causality from LC653 to PC652 is direct whereas the causality from LC653 to PC651 can be considered as indirect.

Consequently, the final causal model illustrating the propagation path of the oscillation is shown in Fig. 9. Note that PC673 does not influence and is neither influenced by any of the investigated controllers, therefore it is not part of the model. Furthermore, the model points on two possible root causes for the fault: PC1652 and PC671 since those are the only controllers that have causal pathways to all the others. Therefore, to locate the root cause in such case, we propose to quantify the level of influence of each controller on the remaining controllers by calculating the sum of all C_{NPMR} values originating from each controller (according to Table 1). The results (Fig. 10) clearly identify ‘PC1652’ as the root cause. Moreover, as expected, the highest C_{NPMR} values are originating in the drying group where the stiction was detected (PC1652, PC671 and LC653) and the values are decreased along the consecutive groups.

Overall, the analysis proved to be highly efficient and accurate in identifying the propagation path. Ultimately, only one causality estimation turned out to be spurious (LC653 → PC651). Misdetection might be attributed to the parameters selection, especially the kernel

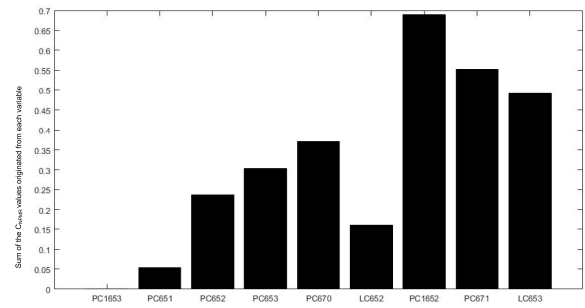


Fig. 10. The sum of all C_{NPMR} values originating from each controller.

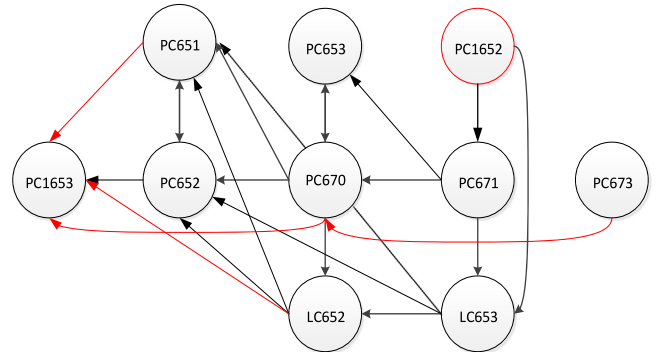


Fig. 11. The causal model obtained with fixed parameters (red arcs correspond to causality which was not obtained with adjusted parameters). (For interpretation of the references to color in this figure legend, the reader is referred to the web version of this article.)

tolerance tuning. When tuning σ , it was observed that even a small variation in σ lead to a significant difference in the corresponding C_{NPMR} value. Moreover, σ has a larger influence on C_{NPMR} than d and τ . Therefore, the optimization of the kernel tolerance remains a challenge for future investigations. Further, although we found that parameters tuning is essential to obtain adequate results, several estimations with different parameters revealed that the causality pattern remains similar and only the amplitude of C_{NPMR} changes, thus resulting in more false positive results. The causality matrix that was obtained with the same methodology but with fixed parameters: $\tau = 1$, $d=4$ and $\sigma = 1$ is shown in Table 4. The values in red correspond to estimations that were excluded when using adjusted parameters (Table 1). The corresponding causal model is shown in Fig. 11 where the red arcs correspond to the values colored in red in Table 4. The results using fixed parameters suggest that the causality pattern is almost unaltered when the parameters are adjusted; however, it is expected to yield more false-positive results (corresponding to the values in red). In addition, it is noteworthy that the causality PC671 → PC1652, which was accurately captured by the analysis with adjusted parameters, was found to be non significant when using fixed parameters, presumably since the directionality in the opposite direction is considerably stronger.

3.5. Comparison to other causality estimators

The NPMR-based estimator has shown several advantages over other causality estimators (Granger causality, frequency domain measures, transfer entropy and nearest neighbors) when applied to the same case study in previous investigations carried out by the authors (Landman & Jämsä-Jounela, 2016, 2018; Landman et al., 2014). Aside from its inherent advantages of being nonparametric and not restricted to linear processes, it showed superior accuracy compared with the transfer entropy and nearest neighbors methods. The results of this study are easier to interpret as all the estimations underwent

Table 4
The NPMR-based causality matrix with fixed parameters $\tau = 1, d = 4, \sigma = 1$.

C_{NPMR} <small>row-column</small>	PC1653	PC651	PC652	PC653	PC670	LC652	PC1652	PC671	LC653	PC673
PC1653										
PC651	0.206		0.269							
PC652	0.213	0.107								
PC653					0.633					
PC670	0.289	0.186	0.192	0.472		0.295				
LC652	0.228	0.082	0.236							
PC1652								0.407	0.588	
PC671				0.498	0.533				0.603	
LC653		0.238	0.275			0.317				
PC673					0.263					

a statistical significance test. Indeed, the final results indicate that the analysis produced one specious causal estimation ($LC653 \rightarrow PC651$) that was initially identified as direct and was eventually established as indirect by calculating the multivariate estimation ($LC653 \rightarrow LC652 \rightarrow PC651$).

Although the transfer entropy and nearest neighbors methods yielded a fairly precise model, the results were evaluated according to their magnitude instead of computationally expensive methods relying on surrogate data (Duan et al., 2014). Furthermore, the two methodologies proposed by the authors for implementing the transfer entropy and nearest neighbors methods are implemented in two phases: bivariate analysis in phase I and multivariate analysis in phase II to discriminate indirect causality. On the other hand, the NPMR-based estimator is applied in a single phase to either bivariate or multivariate estimations without any modifications, thus rendering it highly practical for industrial applications. In addition, the NPMR-based estimator was able to locate the root cause by calculating the sum of C_{NPMR} of each row in the causality matrix. Thereby, the estimator can be easily used to validate or locate the root cause of a fault without using additional measures.

The transfer entropy, nearest neighbors, and the NPMR-based estimator are all nonparametric, nonlinear and require the estimation of several parameters: prediction horizon, time delay and embedding dimension. The procedure for estimating the parameters is roughly similar for all the methods; however, the transfer entropy requires the estimation of joint PDFs, whose complexity increases with the dimensionality of the analysis. Thus, in terms of implementation, the transfer entropy analysis requires more computational time and effort.

The traditional GC method is limited to linear estimations and is based on fitting multivariate AR models; however, it is straightforward to implement and the statistical significance can be easily determined via the F -statistic test (Granger, 1969). Hence, the GC method was able to identify the propagation path with less computational effort than the NPMR-based estimator, however, the frequency domain analysis was essential in order to further exclude ambiguous results and to locate the root cause. These findings are somewhat expected since the relationships between the feedback control loops in the drying section are fairly linear. Thus, in such cases, linear methods should be preferred in order to simplify the analysis.

With respect to the frequency domain methods, the linear PDC and DTF are especially useful when investigating an oscillatory disturbance, owing to their ability to quantify the direct and total energy transfer between time series at each frequency, respectively (Yang & Xiao, 2012). The frequency domain methods can assist in locating the root cause of a fault and discriminating between direct and indirect causality (Landman et al., 2014). The main limitation of the frequency-domain methods is determining the statistical significance using surrogate data; it is computationally heavy, as it requires calculation of a threshold value at each frequency for each measure. Therefore, it is recommended to utilize the frequency domain methods as a supplementary analysis in case of an oscillatory disturbance to gain more insights into the system intrinsic behavior. To sum up, Table 5 compares between different methods for causal analysis based on their implementation to the current case study.

4. Summary and conclusions

This study introduced a methodology for hybrid causal analysis using a nonlinear nonparametric causality estimator. The methodology was successfully demonstrated on an industrial case study involving valve stiction in a board machine. Previously, the NPMR-based causality estimator has been applied in habitat modeling (McCune, 2006, 2011) and on physiological data (Nicolaou & Constantinou, 2016), while this study extended its applicability to industrial processes. The numerous advantages of the NPMR-based estimator render it highly efficient and practical compared with other causality estimators. Furthermore, NPMR-based estimator can be used for identifying the root cause of a fault in case ambiguous results are obtained from the causal model.

The keystone of the proposed methodology is the incorporation of process connectivity information into the causality estimation using a search algorithm. This type of hybrid analysis enables to tackle complex industrial systems while increasing the credibility of the results and reducing the computational effort. Indeed, the results indicate that all of the indirect paths according to the process topology were identified as indirect according to their C_{NPMR} values, while the majority of the paths that were considered as direct according to process topology showed a significant level of causality. This demonstrates the importance of incorporating the process connectivity information into data-based analysis. Nevertheless, the connectivity information is merely a qualitative representation of the process schematic that does not include any information on the process itself, such as chemical composition and reactions rate. Thus, it is problematic, for instance, to retrace the propagation path of a disturbance in a composition of a stream. Thambirajah et al. (2009) and Yim et al. (2006) addressed various limitations of process schematic in their studies and proposed several solutions to solve them. Further research should therefore focus on the development of standardized software that could discover and examine additional information on a process that could enrich the connectivity information (Thambirajah et al., 2009). Another important implication of this study is that setting the appropriate parameters (embedding delay, dimension, kernel tolerance) is highly recommended but not imperative to obtain satisfactory results. Setting the initial parameters based on prior process knowledge (such as the process time delay) could be sufficient to gain an initial model and to locate the root cause. Thereafter, if necessary, the results could be enhanced by tuning the parameters. However, it is recommended that further research be undertaken on the optimization of kernel tolerance due to its effect on the estimation. In particular, it would be interesting to assess the effect of each predictor on the estimation by optimizing the tolerance individually for each predictor.

The major limitation of this study is that it does not include a variety of case studies. Further research is required to establish the efficacy of the proposed causal analysis using other case studies with different types of disturbances. In particular, the performance of the NPMR-based estimator should be examined by considering the following aspects: the level of nonlinearity and complexity of a system, other types of faults and disturbances such as sensor faults, disturbances in unmeasured variables and non-oscillatory disturbances.

Table 5

Comparison between the causality estimators based on the results of the hybrid causal analysis on the board machine.

Method	Results accuracy	Parameters to select	Significance testing	Computational load	Remarks
Granger causality and the frequency domain measures	High ($\approx 88\%$ accuracy)	Model order (AIC criteria)	Yes (F -statistic test for the GC and surrogates for the PDC and DTF)	Low (The significance testing of the PDC and DTF using surrogate data requires high computational effort)	Frequency analysis was used as an auxiliary method to exclude spurious results and identify the root cause.
Transfer Entropy	Good	Embedding dimension, prediction horizon and time delay	No	High	Two phase implementation
Nearest neighbors	High ($\approx 90\%$ accuracy)	Embedding dimension, prediction horizon, time delay and number of nearest neighbors	No	Moderate	Two phase implementation
NPMR-based causality estimator	Very High (The highest among all estimators)	Embedding dimension, time delay and kernel tolerance	Yes (with AAFT surrogates)	Moderate	One phase implementation

The NPMR-based estimator showed superior performance compared with the nonlinear nearest neighbors and transfer entropy methods. On the other hand, the conditional GC was able to produce adequate results with low computational time and effort. These findings suggest that in future cases, straightforward linear methods such as GC should be applied at first to obtain an initial model, especially for small-scale systems with a simple topology. In case of an oscillatory disturbance, the frequency domain measures can be used to identify the root cause and/or exclude spurious results from the model. If the system is highly complex and nonlinear, the NPMR-based estimator would be an appropriate selection. Overall, this study strengthened the idea that in order to handle a large-scale complex system, a reasonable approach would be to combine a topology-based model with data-based analysis or apply several causality estimators in parallel. The work presented in the paper can serve as a basis for the future development of a powerful diagnostic tool for industrial applications. Still and all, it would be highly beneficial to validate the final results using the available process knowledge or site experts.

Declaration of competing interest

The authors declare that they have no known competing financial interests or personal relationships that could have appeared to influence the work reported in this paper.

Acknowledgments

The research leading to these results was funded from the Plantwide eMPC project of the Academy of Finland under agreement No. 13296432. In particular, the authors thank Stora Enso Oyj for providing the data and the expert knowledge for the analysis.

References

- Alcala, C. F., & Qin, S. J. (2009). Reconstruction-based contribution for process monitoring. *Automatica*, 45, 1593–1600.
- Ancona, N., Marinazzo, D., & Stramaglia, S. (2004). Radial basis function approach to nonlinear Granger causality of time series. *Physical Review E*, 70(056221), <http://dx.doi.org/10.1103/PhysRevE.70.056221>.
- Baccala, L. A., & Sameshima, K. (2001). Partial directed coherence: a new concept in neural structure determination. *Biological Cybernetics*, 84, 463–474.
- Bauer, M., Cox, J. W., Caveness, M. H., Downs, J. J., & Thornhill, N. F. (2007). Nearest neighbors methods for root cause analysis of plantwide disturbances. *Industrial and Engineering Chemistry Research*, 46, 5977–5984.
- Bauer, M., & Thornhill, N. F. (2008). A practical method for identifying the propagation path of plant-wide disturbances. *Journal of Process Control*, 18, 707–719.
- Bauer, M., Thornhill, N. F., & Meaburn, A. (2005). Cause and effect analysis of a chemical process analysis of a plant-wide disturbance. In *The IEEE seminar on control loop assessment and diagnosis* (pp. 23–30). London, UK.
- Bressler, S. L., & Seth, A. K. (2011). Wiener-Granger causality: A well established methodology. *NeuroImage*, 58, 323–329.
- Cao, L. (1997). Practical method for determining the minimum embedding dimension of a scalar time series. *Physica D*, 110, 43–50.

- Chen, Y., Rangarajan, G., Feng, J., & Ding, M. (2004). Analyzing multiple nonlinear time series with extended Granger causality. *Physics Letters. A*, 324, 26–35.
- Chen, H.-S., Zhao, C., Yan, Z., & Yao, Y. (2017). Root cause diagnosis of oscillation - type plant faults using nonlinear causality analysis. *IFAC PapersOnLine*, 50, 13898–13903.
- Choudhury, S., Kariwala, V., Thornhill, N. F., Douke, H., Shah, S., Takada, H., et al. (2007). Detection and diagnosis of plant-wide oscillations. *The Canadian Journal of Chemical Engineering*, 85, 208–219.
- Dolan, K. T., & Spano, M. L. (2001). Surrogate for nonlinear time series analysis. *Physical Review E*, 64, 1–6.
- Duan, P., Chen, T., Shah, S., & Yang, F. (2014). Methods for root cause diagnosis of plant-wide oscillations. *AIChE Journal*, 60, 2019–2034.
- Duan, P., Yang, F., Chen, T., & Shah, S. (2013). Direct causality detection via the transfer entropy approach. *IEEE Transactions on Control Systems Technology*, 21, 2052–2066.
- Faes, L., Nollo, G., & Chon, K. (2008). Assessment of Granger causality by nonlinear model identification : application to short-term cardiovascular variability.. *Annals of Biomedical Engineering*, 36, 381–395.
- Fraser, A., & Swinney, H. (1986). Independent coordinates for strange attractors from mutual information. *Physical Review A*, 33, 1134–1140.
- Granger, C. W. J. (1969). Investigating causal relations by econometric models and cross-spectral methods. *Econometrica*, 37, 424–438.
- Guo, S., Seth, A. K., Kendrick, K., Zhou, C., & Feng, J. (2008). Partial Granger causality : eliminating exogenous inputs and latent variables. *Journal of Neuroscience Methods*, 172, 79–93.
- Jämsä-Jounela, S.-L., Tikkanen, V.-M., Zakharov, A., Pozo Garcia, O., Laavi, H., Myller, T., et al. (2012). Outline a fault diagnosis system for a large-scale board machine. *International Journal of Advanced Manufacturing Technology*, 65, 1741–1755.
- Jiang, H., Patwardhan, R., & Shah, S. L. (2008). Root cause diagnosis of plant-wide oscillations using the adjacency matrix. In *The 17th world congress, the international federation of automatic control* (pp. 13893–13900). Seoul, Korea.
- Kaminski, M. J., & Blinowska, K. J. (1991). A new method of the description of the information flow in the brain structures. *Biological Cybernetics*, 65, 203–210.
- Landman, R., & Jämsä-Jounela, S.-L. (2016). Hybrid approach to causal analysis on a complex industrial system based on transfer entropy in conjunction with process connectivity information. *Control Engineering Practice*, 53, 14–23.
- Landman, R., & Jämsä-Jounela, S.-L. (2018). Fault propagation analysis by implementing nearest neighbors method using process connectivity. *IEEE Transactions on Control Systems Technology*, 1–10. <http://dx.doi.org/10.1109/tcst.2018.2847651>.
- Landman, R., Kortela, J., Sun, Q., & Jämsä-Jounela, S.-L. (2014). Fault propagation analysis of oscillation in control loops using data-driven causal analysis and plant connectivity. *Computers & Chemical Engineering*, 71, 446–456.
- Li, G., Qin, S. J., & Yuan, T. (2016). Data-driven root cause diagnosis of faults in process industries. *Chemometrics and Intelligent Laboratory Systems*, 159, 1–11.
- Li, W., Zhao, C., & Huang, B. (2018). Distributed dynamic modeling and monitoring for large-scale industrial processes under closed-loop control. *Industrial and Engineering Chemistry Research*, 57, 15759–15772.
- McCune, B. (2006). Non-parametric habitat models with automatic interactions. *Journal of Vegetation Science*, 17, 819–830.
- McCune, B. (2011). Nonparametric Multiplicative Regression for Habitat Modeling. Technical Report Oregon State University.
- Nicolaou, N., & Constantinou, T. G. (2016). A nonlinear causality estimator based on non-parametric multiplicative regression. *Frontiers in Neuroinformatics*, 10, 1–21.
- Noumenon (2008). XmpLant overview, <https://www.poscaesar.org/svn/pub/PCA/MemberMeeting/200907/2-6-Adrian>.
- Palus, M., & Vejmelka, M. (2007). Directionality of coupling from bivariate time series: How to avoid false causalities and missed connections. *Physical Review E*, 75(056211), 1–14.

- Pozo Garcia, O., Tikkala, V.-M., Zakharov, A., & Jämsä-Jounela, S.-L. (2013). Integrated FDD system for valve stiction in a paperboard machine. *Control Engineering Practice*, 21, 818–828.
- Schreiber, T. (2000). Measuring information transfer. *Physical Review Letters*, 85, 461–464.
- Sun, Q. (2013). Generation of process topology-based causal models, Msc thesis, Espoo, Finland URL <https://aaltodoc.aalto.fi/handle/123456789/11136>.
- Thambirajah, J., Benabbas, L., Bauer, M., & Thornhill, N. F. (2007). Cause and effect analysis in chemical processes utilizing plant connectivity information. In *The IEEE advanced process control applications for industry workshop* (pp. 1–6). Vancouver, Canada.
- Thambirajah, J., Benabbas, L., Bauer, M., & Thornhill, N. F. (2009). Cause-and-effect analysis in chemical processes utilizing xml, plant connectivity and quantitative process history. *Computers and Chemical Engineering*, 33, 503–512.
- Theiler, J., Eubank, S., Longtin, A., Galdrikian, B., & Farmer, J. D. (1992). Testing for nonlinearity in time series- the method of surrogate data. *Physica D*, 58, 77–94.
- Thornhill, N. F., Cox, J. W., & Paulonis, M. A. (2003). Diagnosis of plant-wide oscillation through data-driven analysis and process understanding. *Control Engineering Practice*, 11, 1481–1490.
- Thornhill, N. F., & Horch, A. (2007). Advances and new directions in plant-wide disturbance detection and diagnosis. *Control Engineering Practice*, 15, 1196–1206.
- Vakorin, V., Krakovska, O., & McIntosh, A. (2009). Confounding effects of indirect connections on causality estimation. *Journal of Neuroscience Methods*, 184, 152–160.
- Venkatasubramanian, V., Rengaswamy, R., Yin, K., & Kavuri, S. N. (2003). A review of process fault detection and diagnosis: Part i: Quantitative model-based methods. *Computers and Chemical Engineering*, 27, 293–311.
- Yan, Z., & Yao, Y. (2015). Variable selection method for fault isolation using least absolute shrinkage and selection operator (lasso). *Chemometrics and Intelligent Laboratory Systems*, 24, 450–459.
- Yang, F., Duan, P., Shah, S. L., & Chen, T. (2014). *Capturing connectivity and causality in complex industrial processes*. Springer.
- Yang, F., Shah, S. L., & Xiao, D. (2012). Signed directed graph based modeling and its validation from process knowledge and process data. *International Journal of Applied Mathematics and Computr Science*, 22, 387–392.
- Yang, F., & Xiao, D. (2012). Progress in root cause and fault propagation analysis of large-scale industrial processes. *Journal of Control Science and Engineering*, 2012, 1–10.
- Yim, S., Ananthakumar, H. G., Benabbas, L., Horch, A., Drath, R., & Thornhill, N. F. (2006). Using process topology in plant-wide control loop performance assessment. *Computers and Chemical Engineering*, 31, 86–99.
- Yu, W., & Zhao, C. (2018). Sparse exponential discriminant analysis and its application to fault diagnosis. *IEEE Transactions on Industrial Electronics*, 65, 5931–5940.
- Yuan, T., & Qin, S. J. (2013). Root cause diagnosis of plant-wide oscillations using granger causality. In *The 8th IFAC symposium on advanced control of chemical processes* (pp. 160–165). Singapore: The international Federation of Automatic Control.
- Zakharov, A., Zattoni, E., Xie, L., Pozo Garcia, O., & Jämsä-Jounela, S.-L. (2013). An autonomous valve stiction detection system based on data characterization. *Control Engineering Practice*, 21, 1507–1518.
- Zhao, C., & Sun, H. (2019). Dynamic distributed monitoring strategy for large-scale nonstationary processes subject to frequent varying conditions under closed-loop control. *IEEE Transactions on Industrial Electronics*, 66, 4749–4758.
- Zhao, C., & Wang, W. (2016). Efficient faulty variable selection and parsimonious reconstruction modelling for fault isolation. *Journal of Process Control*, 38, 31–41.